Journal of Biomedical Optics

SPIEDigitalLibrary.org/jbo

Double-pass Mach–Zehnder fiber interferometer pH sensor

Zhi Qiang Tou
Chi Chiu Chan
Jesmond Hong
Shermaine Png
Khay Ming Tan Eddie
Terence Aik Huang Tan

SPIE

Double-pass Mach–Zehnder fiber interferometer pH sensor

Zhi Qiang Tou,[a] Chi Chiu Chan,[a,*] Jesmond Hong,[a] Shermaine Png,[a] Khay Ming Tan Eddie,[b] and Terence Aik Huang Tan[a]
[a]Nanyang Technological University, School of Chemical and Biomedical Engineering, Division of Bioengineering, 70 Nanyang Drive, Singapore 637457, Singapore
[b]EINST Technology Pte Ltd, 1092 Lower Delta Road #04-01, Singapore 169203, Singapore

Abstract. A biocompatible fiber-optic pH sensor based on a unique double-pass Mach–Zehnder interferometer is proposed. pH responsive poly(2-hydroxyethyl methacrylate-co-2-(dimethylamino)ethyl methacrylate) hydrogel coating on the fiber swells/deswells in response to local pH, leading to refractive index changes that manifest as shifting of interference dips in the optical spectrum. The pH sensor is tested in spiked phosphate buffer saline and demonstrates high sensitivity of 1.71 nm/pH, pH 0.004 limit of detection with good responsiveness, repeatability, and stability. The proposed sensor has been successfully applied in monitoring the media pH in cell culture experiments to investigate the relationship between pH and cancer cell growth. © *2014 Society of Photo-Optical Instrumentation Engineers (SPIE)* [DOI: 10.1117/1.JBO.19.4.047002]

Keywords: fiber optic sensors; interferometers; remote sensing; pH.

Paper 130862R received Dec. 4, 2013; revised manuscript received Mar. 14, 2014; accepted for publication Mar. 17, 2014; published online Apr. 10, 2014.

1 Introduction

pH plays an important role in many biochemical reactions, which makes its monitoring and regulation fundamental in many fields. In cancer studies, for instance, the extracellular pH is thought to impact the invasive behavior of tumor cells,[1] control activity of tumor-infiltrating T lymphocytes[2] among other roles, making its determination crucial for predicting cancer cell progression and deciding a suitable antitumor therapy.[3]

Although the conventional glass electrode pH meter remains the gold standard for pH measurements, it is bulky and requires regular calibration that limits its usefulness for continuous monitoring. Establishing a pH sensor on a fiber optic platform can offer numerous advantages unique to fiber optics, including miniature size, immunity to electromagnetic interference, and capability for multiplex, remote sensing. Fiber optic pH meters have been reported,[4,5] with the vast majority based on the fluorescence or absorbance of pH responsive dyes entrapped on distal end of optical fibers, rendering them vulnerable to inaccuracies arising from light source fluctuations, photobleaching, and leaching.

Fiber sensors based on interferometry have emerged recently, with novel configurations being reported for a wide varying range of applications and are touted to give remarkable performance in terms of sensitivity, accuracy, and dynamic range.[6] In interferometry, a coherent light is split into two paths: a reference path and a sample path that interacts with the measurand. Due to the interaction, light accumulates a phase difference with respect to light propagating in the reference path, creating an interferogram when light from both paths are recombined. Any change in the measurand alters the phase difference and manifests as a phase shift of the interferogram. Since spectral shift instead of light intensity is measured, the interferometer sensor is insensitive to many problems that plague fluorescence based sensors.

In this paper, we propose a double-pass Mach–Zehnder fiber interferometer based on a short segment of photonic crystal fiber (PCF) fusion spliced in between single-mode fiber (SMF) similar to Refs. 7 and 8. The splice joints serve as a coupler to split light into the PCF's core mode and cladding modes as it passes toward the PCF segment and to recombine the core and cladding modes as light leaves the PCF segment. A silver mirror is coated on the distal end of the fiber to reflect light which is made to transverse the PCF segment a second time.

pH sensitivity is conferred to the fiber sensor by coating the latter with a layer of poly(2-hydroxyethyl methacrylate-co-2-(dimethylamino)ethyl methacrylate) pH responsive hydrogel film. The pH responsive hydrogel is a three-dimensional hydrophilic polymer network structure[9] that exhibits a distinctive volume phase transition in response to pH.[10] Our experimental results have demonstrated that the pH fiber sensor exhibits a good sensitivity to pH changes within the physiological range along with good repeatability, responsiveness. In addition, we have also demonstrated the capability of the sensor for *in vitro* monitoring of media pH in cell culture experiments. The promising results pave the way for using hydrogel coated interferometry based pH sensors for *in-vivo* applications.

2 Materials and Methods

2.1 *Materials*

Optical fibers including SMF and PCF (10.1/125 μm LMA-10) are purchased from Corning, (New York) and NKT Photonics, (Birkerød, Denmark), respectively.

Anhydrous methanol, sodium hydroxide granules, silver nitrate, 2-hydroxyethyl methacrylate (HEMA), 2-(dimethylamino)ethyl methacrylate (DMAEM), and ethylene glycol

*Address all correspondence to: C. C. Chan, E-mail: ECCChan@ntu.edu.sg

dimethacrylate (EGDMA) are purchased from Alfa Aesar, (Massachusetts) and glucose, tin dichloride 3-(trimethoxysilyl)propyl methacrylate (TMSPM) and N, N, N', N'-tetramethylethylenediamine (TEMED), inhibitor removers and ammonium persulfate (APS) are procured from Sigma, (St. Louis, Missouri). Sulfuric acid (95% to 97%) and hydrogen peroxide (30%) are from Merck, (New Jersey) and VWR, (Pennsylvania), respectively.

All reagents are of analytical grade and solutions are prepared using ultrapure water with resistivity 18.2 MΩ cm from Milli-Q system.

2.2 *Methods*

2.2.1 *Preparation of Mach–Zehnder fiber interferometer*

LMA-10 is a PCF in which light is confined within a 10.1 μm solid core via a regular hexagonal lattice array of air holes surrounding the core.

A segment of LMA-10 is fusion spliced in between SMFs using an electric arc splicer (Type 39, Sumitomo, Tokyo, Japan). All fiber ends are cleaved using a precision fiber cleaver (Fujikura, Tokyo, Japan, CT-30) prior to splicing. The fiber ends are aligned manually based on the fibers' edge and an electric arc is applied to join the fibers while simultaneously collapsing the LMA-10's air holes at the splicing joint.

2.2.2 *Surface modification of LMA-10*

The LMA-10 surface is hydroxylated by immersing in piranha solution (sulfuric acid and hydrogen peroxide) in 7:3 volume ratio at 80°C for an hour, followed by thorough rinsing with deionized water and drying under stream of nitrogen gas.

The fibers are then silanized by immersion in 10 v/v % TMSPM prepared in anhydrous methanol for 4 h and sequentially rinsed with methanol and water before leaving to dry overnight in the dark.

2.2.3 *Coating of silver mirror at fiber tip*

The silver mirror is coated using procedures adapted from Wang et al.[11] The piranha solution treated fiber tip is immersed in 8 wt/v % aqueous sodium hydroxide followed by 5 wt/v % tin dichloride to promote silver binding. A 2 wt/v % silver nitrate solution is prepared and aqueous ammonia is added drop wise until the solution just turns clear colorless. The fiber tip is dipped in a final solution consisting the prepared silver nitrate solution and 4 wt/v % glucose solution in a 5:3 volume ratio for 2 h after which it is rinsed with deionized water and dried under nitrogen stream.

2.2.4 *Coating of pH-responsive gel on fiber surface*

HEMA and DMAEM are treated with inhibitor removers prior to use. HEMA, DMAEM, EGDMA, and water are mixed to obtain the pregel solution. The amount of EGDMA, which is used as the cross-linker, is kept at 5 mol %. The total wt/v % of monomers is kept at 60%. The pregel solution is degassed by bubbling nitrogen gas for 20 min.

Free radical polymerization is initiated via addition of APS and TEMED (0.05 wt/v % and 0.10 wt/v % of final volume, respectively). The fibers are affixed separately in custom-made polydimethylsiloxane (PDMS) channels. The pregel is injected into the channels and left overnight in a vacuum oven. The fibers are then removed from the channels and immersed in deionized water to remove any unreacted materials from the hydrogel.

2.2.5 *Cell culture experiment*

A-375 melanoma cells are obtained from ATCC and cultured using Dulbecco's modified Eagle medium (Life Technologies, California, Gibco 10566 with 10 v/v % fetal bovine serum (Life Technologies, California, Gibco 10270) and 1 v/v % penicillin streptomysin (Life Technologies, California, Gibco 15140) in an incubator maintained at 37°C and a 5% carbon dioxide atmosphere.

An initial 25,000 cells are seeded in a 24-well plate. The cell proliferation and pH of the culture medium are monitored daily over 7 days. The pH of the medium is measured both by the proposed optical fiber sensor and a conventional glass electrode pH meter (Jenway, Staffordshire, United Kingdom, Model 3510). Cell proliferation is monitored by trypsin (Biological Industries, Kibbutz Beit-Haemek, Israel) treatment followed

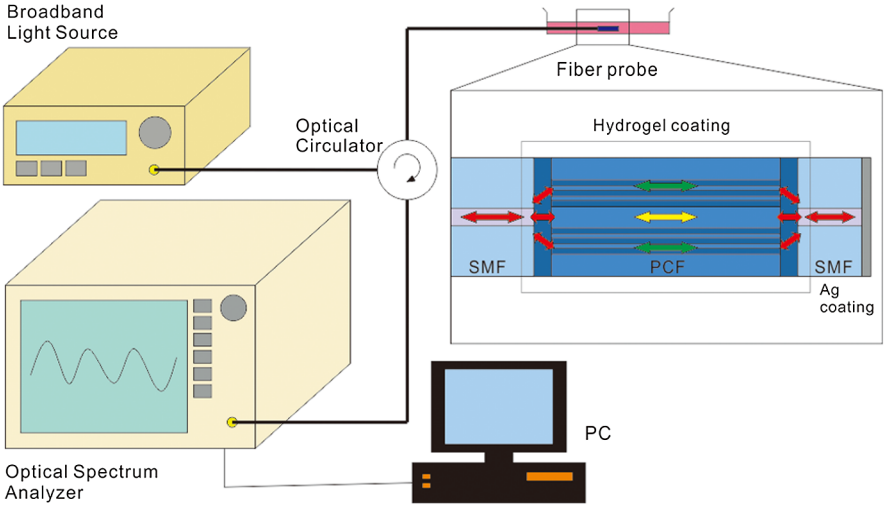

Fig. 1 Schematic of the experimental setup. The LMA-10 core and cladding modes are represented by yellow and green arrows, respectively.

by cell counting in a hemocytometer using trypan blue (Life Technologies, California, Gibco 15250) staining.

2.2.6 *Experimental setup*

Broadband light source (AS3223-BA2) with emission wavelength from 1530 to 1605 nm is used to interrogate the fiber sensor with the reflected light detected by an optical spectrum analyzer (AQ6370, Yokogawa, Tokyo, Japan) via an optical circulator as outlined in Fig. 1. The reflection spectra are recorded and further processed using MATLAB. pH response is characterized by immersing the pH sensor in phosphate buffer saline spiked with aqueous hydrochloric acid or sodium hydroxide.

3 Results and Discussion

3.1 *Single-Pass Versus Double-Pass Fiber Interferometer*

The proposed sensor improves on the single-pass Mach–Zehnder interferometer previously reported.[7,8] The fundamental optical mode guided by LMA-10 is a quasi-Gaussian mode with mode field diameter 8.8 μm (@1064 nm) which makes it confined within the optical fiber's core and is thus termed the core mode. The collapsed air holes at the splice joint represent a region of uniform refractive index where the light guidance is lost. As a result, the guided mode of the SMF diffracts and broadens as it transverses the collapsed region to LMA-10. The extent of broadening can be estimated from Gaussian beam approximation[12] and the broadened beam excites fundamental mode and higher-order modes of LMA-10. These higher-order modes suffer from high optical losses and have significant energies propagating within the structured cladding of the LMA-10 and are commonly termed as cladding modes.

A second collapsed region serves to recombine the LMA-10's core and cladding modes into the core mode of the ensuing SMF. Since the core and cladding modes have different propagation constants, they recombine to produce an interference pattern that is commonly described by a two-beam interference (between a core and cladding mode) model:[7]

$$I_{\text{interference}} = I_{\text{core}} + I_{\text{clad}} + 2\sqrt{I_{\text{core}} + I_{\text{clad}}}\,\cos[k(n_{\text{eff-core}} - n_{\text{eff-clad}})L],$$

where I_{core}, I_{clad}, k, $n_{\text{eff-core}}$, $n_{\text{eff-clad}}$, and L are the intensity of the core mode, intensity of the cladding mode, wave number, effective refractive index of the core mode, effective refractive index of the cladding mode, and interferometer length, respectively.

Since the cladding modes propagate by reflection off the fiber cladding-exterior interface, their effective refractive indices are affected by the exterior refractive index while the core mode, due to its confinement within the fiber core, remains relatively insensitive to the exterior. As a result, a change in exterior refractive index alters the phase difference between the core and cladding modes leading to a phase shift in $I_{\text{interference}}$ that may be characterized by the amount of shifting of the interference dips.

A common drawback of the Mach–Zehnder interferometer is the inverse relationship between the interferometer length and the free spectral range (FSR) of the interference pattern.[13] A longer interferometer, while able to give higher sensitivity through a larger optical path length difference, decreases the FSR, thus limiting dynamic range. We seek to mitigate this problem by coating a silver mirror at the interferometer end so that the light propagates through the interferometer twice. This also turns the interferometer into a probe device that is more convenient for sensing application. Figure 2 shows the interference pattern for a double-pass and single-pass Mach–Zehnder interferometer with the inset monitoring the spectral position of an interference dip with change in external refractive index. Although there is no significant improvement in sensitivity, larger fringe contrast is observed in the interferogram of the double-pass interferometer. Peak-to-peak values normalized with respect to the FSR were 0.863 and 0.444 for double-pass and single-pass interferometer, respectively, hence the quality factor, Q, of the interferometer is improved.[14]

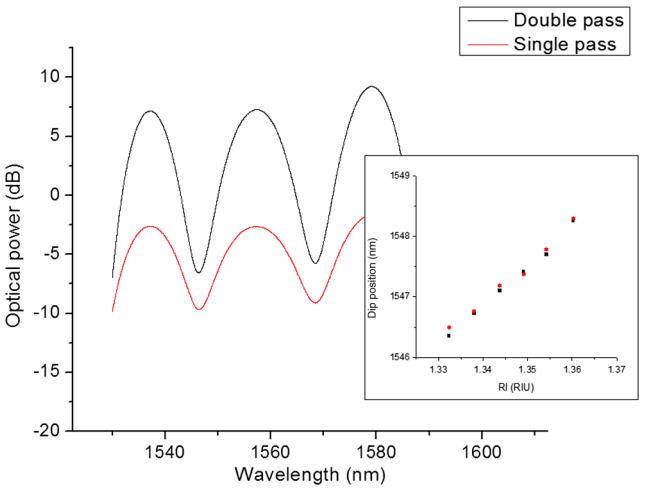

Fig. 2 Spectra of double-pass and single-pass interferometers. (inset) Monitoring of spectra dip shifts with changes in external refractive indices.

3.2 *Coating pH Responsive Hydrogel*

Optical fibers are first silanized with TMSPM to modify the surface with vinyl group for chemical attachment with the pH responsive hydrogel. The hydrogel is formed by *in-situ* free radical initiated polymerization process from pregel mixture of the constituent monomers, cross–linkers, and initiators. The relative amount of monomers, cross-linkers, and initiator influences the morphology and structure of the hydrogel which in turns affects its swelling/deswelling characteristics. A major challenge lies in the reproducible coating of a thin uniform hydrogel film on the optical fiber. A thin film is desirable since the swelling and deswelling are, in part, a diffusion driven process and thicker film would degrade responsiveness of the sensor. Surface initiated polymerization that immobilizes initiator on the surface to fabricate ultrathin hydrogel films (5 to 100 nm) have been reported[15] but is cumbersome to implement on optical fibers as it requires additional chemical modification steps. By carrying out the polymerization process in custom-made PDMS channels, a uniform hydrogel film several micrometers in thickness surrounding the optical fiber can be formed. The thickness of the hydrogel coating extends beyond the penetration depth of the evanescent field of cladding modes (several hundreds of nanometers); hence, the sensor is sensitive to refractive index changes of the

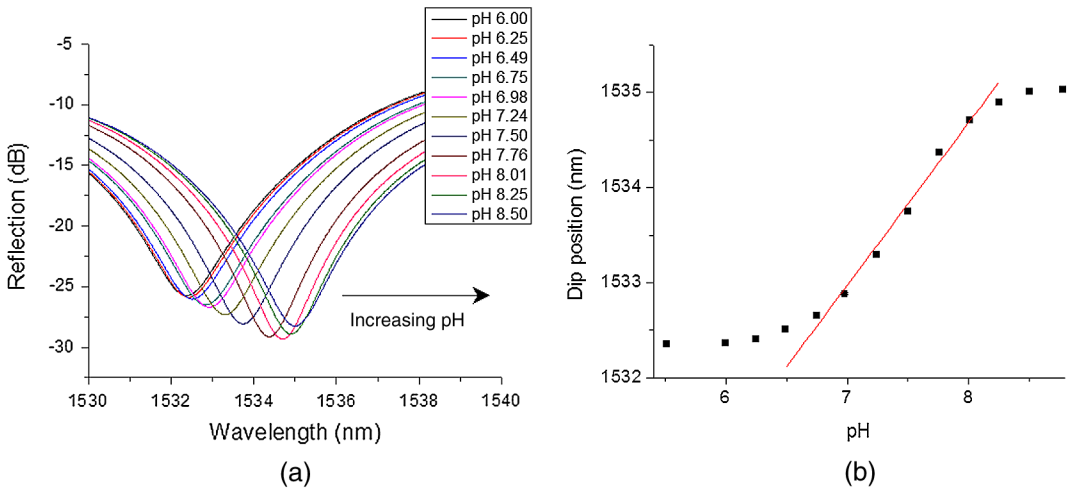

Fig. 3 (a) Interferogram at varying pH in phosphate buffered saline. (b) Corresponding spectral dip position.

hydrogel coating but remains relatively insensitive to thickness change in the hydrogel coating.

3.3 *pH Response in Spiked Phosphate Buffered Saline*

The interference spectra of the pH probe while immersed in phosphate buffered saline (PBS) of varying pH are shown in Fig. 3 with the corresponding shift in interference dip positions. The dip positions are obtained using a MATLAB script that locates dips based on the first derivative of spectra data. It is observed that the spectral dip consistently shifts to longer wavelength when the pH is increased from 5 to 9.

This behavior is attributed to the swelling/deswelling behavior of the hydrogel in response to pH changes. The hydrogel, having a higher refractive index than the solution, increases the refractive index at the fiber surface when it deswells. This increases the effective index of the cladding modes, causing the interference pattern to shift toward longer wavelength. Similarly, a decrease in refractive index at the fiber surface occurs when the hydrogel swells, resulting in the shift of interference pattern toward shorter wavelength.

The pH-dependent swelling and deswelling of the hydrogel are studied at the bulk level by monitoring mass and refractive index change of a hydrogel slab. The hydrogel slab is polymerized from 1 ml of pregel solution with composition outlined in Sec. 2.2.4. The solution is dispensed into a 50-mm diameter Petri dish and APS/TEMED is added to initiate polymerization in a vacuum chamber. The hydrogel thus formed is immersed in deionized water for 2 days and cut into a rectangular slab. The mass of the hydrogel slab is measured using a microquartz balance (Mx5, Mettler Toledo, Ohio) after immersing in PBS of the studied pH for 24 h and drying with a lint free cloth. Refractive indices are measured using with an Abbe refractometer (ATAGO, Tokyo, Japan NAR-4T Solid) using glycerol (Sigma, St. Louis, Missouri, RI 1.4695) as contact liquid. Dry mass of the hydrogel was measured after heating at 40°C in a vacuum chamber overnight.

The mass swell ratio, defined as the ratio of the swollen hydrogel slab over its dry mass, is 1.78 and 1.55 in pH 5 and pH 9 buffer solutions, respectively. This represents a 15% mass difference between the mass of the hydrogel under acidic and alkaline conditions. The increased mass in acidic medium corresponds to swelling of the hydrogel network leading to the increased water content. The increased water content reduces the refractive index of the hydrogel as water has a lower refractive index (RI 1.33) than the polymer [RI of poly(2-hydroxyethyl methacrylate) is approximately 1.51]. The refractive index of the hydrogel in pH 5 is 1.39 and increases to 1.42 when the pH is increased to 9. This is still lower than the refractive index of material for the optical fiber (silica, RI ~ 1.4457), enabling propagation of cladding modes even when the hydrogel is collapsed at high pH.

This swelling/deswelling behavior of the hydrogels is described previously by thermodynamic theories which treat swollen gel as a polymer solution of an analogous linear polymer in a solvent.[16,17] Polymer-solvent interactions, governed by thermodynamic variables, determine the mixing tendency between polymer and solvent responsible for driving solvent into the gel, thus exerting an expansion force that is opposed by an elastic retractive force exerted by polymer chains between the cross-links. An equilibrium swelling state is reached when expansion force balances the retractive force.

pH responsive gel incorporates ionizable acidic or basic groups that alter their swelling behavior. The ionization state of these groups is affected by local pH and changes the charge density within the gel. Here, DMAEM is copolymerized with HEMA with the former contributing basic amino groups to the gel network. Under acidic conditions, protonation of the amino groups within the gel leads to an increased charge density. Electrostatic repulsion between the charged groups causes the expansion of the gel network. In addition, diffusion of counter ions from the solution to balance the internal charges also increases the osmotic pressure within the gel and contributes to gel swelling. The equilibrium swelling of pH responsive gel has been modeled by various groups and found to depend on charge of the ionic monomer, pK_a of the ionizable group, mole ratio of ionizable monomer, degree of cross-linking, and nature of surrounding solvent.[18]

The graph in Fig. 3 assumes a typical sigmoidal titration curve with an apparent pK_a value fitted to be 7.31. This is approximately 1.1 pH units lower than the pK_a of DMAEM in solution[19] as more acidic condition is required to protonate DMAEM in the polymeric form owning to unfavorable electrostatic interactions.[20] The apparent pK_a is close to

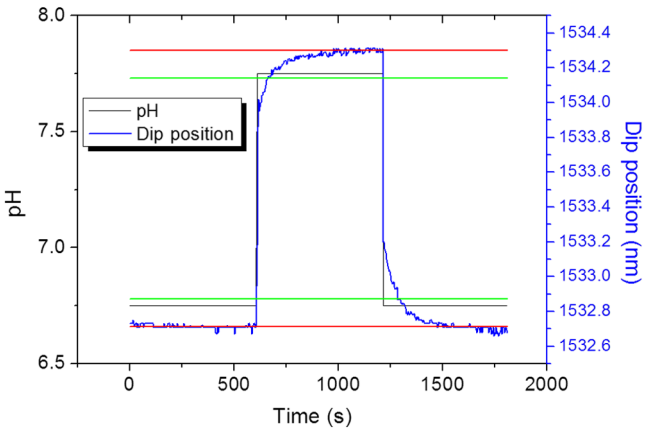

Fig. 4 Step response of fiber sensor from pH 6.75 to pH 7.75.

physiological pH of pH 7.4, making it apt for physiological measurements due to its high sensitivity around the physiological pH.

A linear regression line can be used to fit the pH range: pH 6.75 to 8.25 with r^2 value of 0.986. The pH sensitivity within this linear range is 1.71 nm/pH, which is higher than reported sensors using pH sensitive polyelectrolyte multilayers.[21,22] The limit of detection based on ratio of sensitivity over 3σ, where σ is the standard deviation of five readings, is pH 0.004.

3.4 *Responsiveness of the pH Sensor*

The responsiveness of the proposed pH sensor is tested by allowing the sensor to equilibrate in spiked PBS of pH 6.75 before changing to a spiked PBS of pH 7.75 (Fig. 4). The solution is changed to pH 6.75 spiked PBS following equilibrium at the higher pH.

The time taken to reach 90% response, τ_{90}, is measured to be 55 s for change to higher pH and 79 s for change to lower pH. This responsiveness is slightly improved over other reported hydrogel based pH sensor[23] and is in part due to the robustness of an optical based sensing platform. The diffusion of protons through the hydrogel matrix plays an important role in the kinetics of gel swelling/deswelling,[24] thus thinner gel with larger mesh size are thought to be more responsive. The responsiveness of our sensor could be further increased by decreasing the gel thickness. Nevertheless, the responsiveness of the sensor is sufficient to investigate most biological processes.

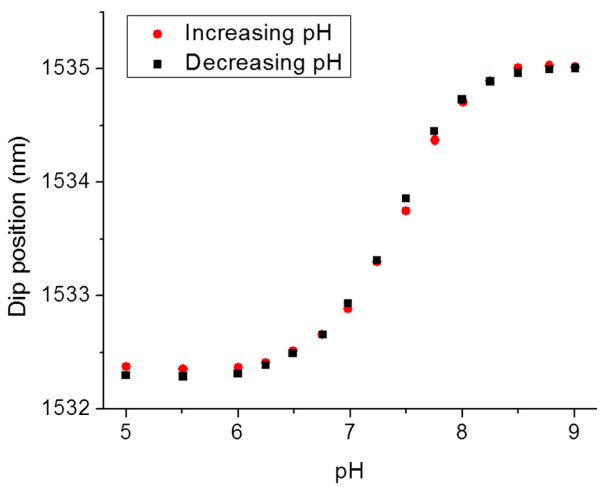

Fig. 5 Sensor pH response under cyclic pH change.

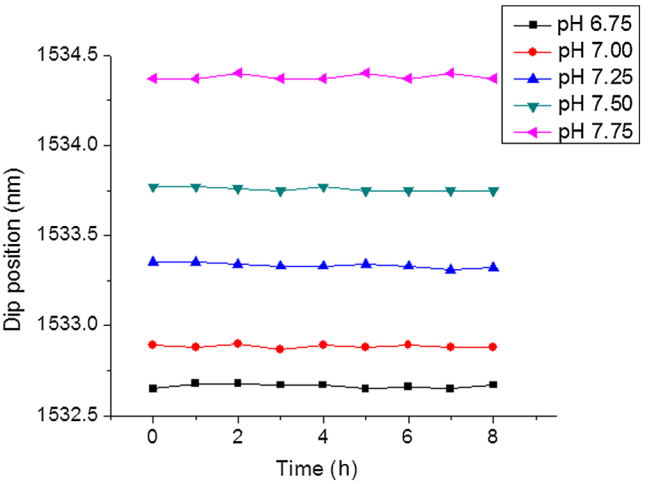

Fig. 6 Stability of pH sensor.

3.5 *Hysteresis of the pH Sensor*

The pH sensor is subjected to cyclic changes in pH to test for its repeatability which is essential for practical usage (Fig. 5). The reversible swelling and deswelling of HEMA-co-DMAEM hydrogel ensures minimal hysteresis with largest reported error of 0.8%.

3.6 *Stability of the pH Sensor*

The stability of the sensor is tested over an 8-h period. Figure 6 shows the sensor performance with minimal fluctuations in PBS of varying pH. The maximum deviation is 0.04 nm corresponding to pH 0.0234 units. Therefore, the proposed sensor has minimal drifting and do not require frequent recalibration that is common for conventional glass electrode pH meter, making the sensor suitable for continuous pH monitoring.

3.7 *Application of the pH Sensor for Cell Culture Monitoring*

Extracellular pH is among the most important parameter influencing cell health and growth and is thus closely monitored in cell culture experiments. The unique demands for continuous monitoring over time under a sterile enclosed environment in typical cell cultures render the conventional glass electrode pH meter inadequate owning to its bulkiness and need for regular calibration and maintenance.

The proposed pH sensor poses several advantages like its miniature size. The use of HEMA as the backbone of the pH responsive gel ensures good biocompatibility, resistance to degradation and allows the sensor to undergo heat sterilization without sustaining damage.

The fiber pH sensor is calibrated in spiked culture media prior to measurement. Figure 7 illustrates the pH change in the culture media measured by our fiber pH sensor and conventional pH meter, highlighting the close proximity between readings from both devices with an average 0.465% error. The media pH is noted to drop drastically from Day 3 corresponding to a sharp increase in cell number before stabilizing at around pH 6.8

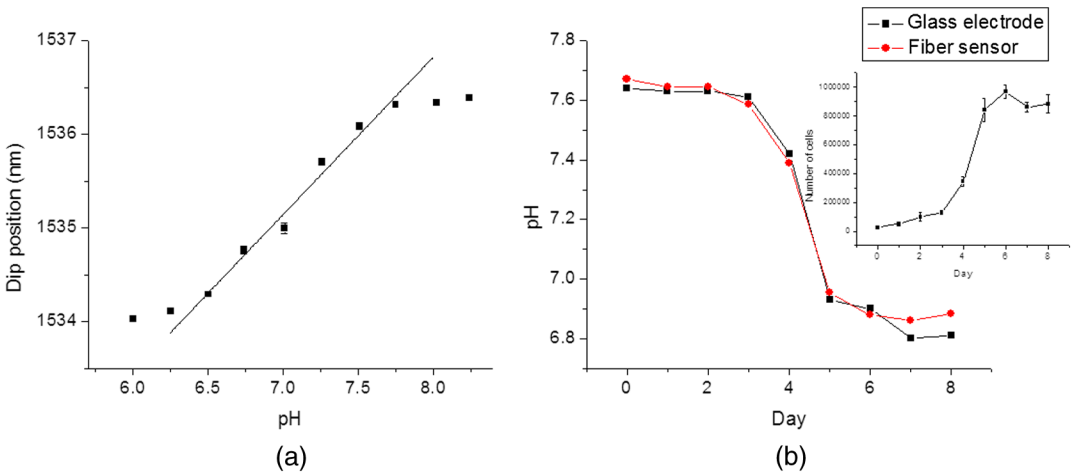

Fig. 7 (a) Calibration of pH sensor in Dulbecco's modified Eagle medium. Fitting of linear regression line between pH 6.50 and pH 7.75 with r^2 value of 0.9762. (b) Monitoring of cell culture pH using fiber pH sensor and glass electrode pH meter. Inset: Monitoring of cell proliferation.

from Day 5. Cell death rate is below 10% throughout the duration of the experiment.

The data agrees with reported pH 6.5 to 6.7 in *in-vivo* studies of tumor microenvironment.[3] The acidic microenvironment that has become characteristic of tumor is the result of increased metabolic activities and a shift in cellular metabolism in response to hypoxia or in part, to confer competitive advantage over normal cells that are intolerant to acidity.[25] The fall in pH is also part of a malignant progression and favors upregulation of proteolytic enzymes that drives metastasis.[26] Clearly, pH is vital in cancer studies and our proposed sensor can be useful *in-vitro* studies to understand cancer or evaluate pH targeted cancer therapies.

4 Conclusions

A fiber optic pH sensor has been demonstrated by coating a pH responsive HEMA-co-DMAEM hydrogel on a double-pass Mach–Zehnder interferometer and successfully applied in a cell culture experiment to monitor media pH.

The proposed pH sensor has a linear pH response between pH 6.75 and 8.25. The dynamic range of sensor can possibly be widened by using an array of such sensors in a spatial division multiplex (SDM) system.[27] Each sensor in the array can be coated with a different pH responsive hydrogel that enables pH sensitivity in a specific range.

To date, hydrogels responsive to various stimuli ranging from the physical such as temperature[28] to chemical such as pH,[29] heavy metal ion,[30] and bio/chemical molecules[31] have been developed and fiber interferometer proves a viable platform for various hydrogel-based sensors. The development of an SDM system of hydrogel based optical interferometer sensors could prove viable for a multi parameter sensing system for biomedical applications.

Acknowledgments

The authors would like to thank Mr. Nishanth for fabrication of the PDMS chip used for hydrogel coating.

References

1. R. Martinez Zaguilan et al., "Acidic pH enhances the invasive behavior of human melanoma cells," *Clin. Exp. Metastasis* **14**(2), 176–186 (1996).
2. A. Calcinotto et al., "Modulation of microenvironment acidity reverses anergy in human and murine tumor-infiltrating T lymphocytes," *Cancer Res.* **72**(11), 2746–2756 (2012).
3. R. J. Gillies et al., "MRI of the tumor microenvironment," *J. Magn. Reson. Imaging* **16**(4), 430–450 (2002).
4. W. Z. Jin et al., "Continuous intra-arterial blood pH monitoring by a fiber-optic fluorosensor," *IEEE Trans. Biomed. Eng.* **58**(5), 1232–1238 (2011).
5. S. A. Grant et al., "In vitro and in vivo measurements of fiber optic and electrochemical sensors to monitor brain tissue pH," *Sens. Actuators, B* **72**(2), 174–179 (2001).
6. B. H. Lee et al., "Interferometric fiber optic sensors," *Sensors* **12**(3), 2467–2486 (2012).
7. H. Y. Choi et al., "All-fiber Mach–Zehnder type interferometers formed in photonic crystal fiber," *Opt. Express* **15**(9), 5711–5720 (2007).
8. J. N. Wang and J. L. Tang, "Photonic crystal fiber Mach–Zehnder interferometer for refractive index sensing," *Sensors* **12**(3), 2983–2995 (2012).
9. K. Deligkaris et al., "Hydrogel-based devices for biomedical applications," *Sens. Actuators, B* **147**(2), 765–774 (2010).
10. D. Buenger et al., "Hydrogels in sensing applications," *Prog. Polym. Sci.* **37**(12), 1678–1719 (2012).
11. S. Q. Wang et al., "Silver-coated near field optical scanning microscope probes fabricated by silver mirror reaction," *Appl. Phys., B* **92**(1), 49–52 (2008).
12. J. Villatoro et al., "Simple all-microstructured-optical-fiber interferometer built via fusion splicing," *Opt. Express* **15**(4), 1491–1496 (2007).
13. D. Wu et al., "Refractive index sensing based on Mach–Zehnder interferometer formed by three cascaded single-mode fiber tapers," *Appl. Opt.* **50**(11), 1548–1553 (2011).
14. Y. Geng et al., "A cascaded photonic crystal fiber Mach–Zehnder interferometer formed by extra electric arc discharges," *Appl. Phys., B* **102**(3), 595–599 (2011).
15. D. J. Kim et al., "Formation of thermoresponsive gold nanoparticle/PNIPAAm hybrids by surface-initiated, atom transfer radical polymerization in aqueous media," *Macromol. Chem. Phys.* **206**(19), 1941–1946 (2005).
16. P. J. Flory, "Thermodynamics of high polymer solutions," *J. Chem. Phys.* **9**(8), 660–661 (1941).
17. M. L. Huggins, "Solutions of long chain compounds," *J. Chem. Phys.* **9**(5), 440–440 (1941).
18. L. Brannonpeppas and N. A. Peppas, "Equilibrium swelling behavior of pH-sensitive hydrogels," *Chem. Eng. Sci.* **46**(3), 715–722 (1991).
19. A. J. Marshall et al., "pH-sensitive holographic sensors," *Anal. Chem.* **75**(17), 4423–4431 (2003).
20. S. Wen et al., "Preparation and characterization of polyelectrolyte copolymers containing methyl-methacrylate, and 2-hydroxyethyl

methacrylate. 2. Polymers based on dimethylaminoethyl methacrylate," *J. Appl. Polym. Sci.* **43**(1), 205–212 (1991).
21. M. J. Yin et al., "Highly sensitive and fast responsive fiber-optic modal interferometric pH sensor based on polyelectrolyte complex and polyelectrolyte self-assembled nanocoating," *Anal. Bioanal. Chem.* **399**(10), 3623–3631 (2011).
22. B. Gu et al., "Low-cost high-performance fiber-optic pH sensor based on thin-core fiber modal interferometer," *Opt. Express* **17**(25), 22296–22302 (2009).
23. A. Richter et al., "Review on hydrogel-based pH sensors and microsensors," *Sensors* **8**(1), 561–581 (2008).
24. Y. Chu et al., "pH-induced swelling kinetics of polyelectrolyte hydrogels," *J. Appl. Polym. Sci.* **58**(12), 2161–2176 (1995).
25. D. Lipson et al., "Multifiber, multiwavelength, fiber optic fluorescence spectrophotometer," *IEEE Trans. Biomed. Eng.* **39**(9), 886–892 (1992).
26. R. E. Moellering et al., "Acid treatment of melanoma cells selects for invasive phenotypes," *Clin. Exp. Metastasis* **25**(4), 411–425 (2008).
27. E. K. Rofstad et al., "Acidic extracellular pH promotes experimental metastasis of human melanoma cells in athymic nude mice," *Cancer Res.* **66**(13), 6699–6707 (2006).
28. J. H. Kang et al., "Thermoresponsive hydrogel photonic crystals by three-dimensional holographic lithography," *Adv. Mater.* **20**(16), 3061–3065 (2008).
29. C. E. Reese et al., "Development of an intelligent polymerized crystalline colloidal array colorimetric reagent," *Anal. Chem.* **73**(21), 5038–5042 (2001).
30. A. Baeissa et al., "DNA-functionalized monolithic hydrogels and gold nanoparticles for colorimetric DNA detection," *ACS Appl. Mater. Interfaces* **2**(12), 3594–3600 (2010).
31. P. T. Charles et al., "Fabrication and characterization of 3D hydrogel microarrays to measure antigenicity and antibody functionality for biosensor applications," *Biosens. Bioelectron.* **20**(4), 53–764 (2004).

Zhi Qiang Tou is a PhD candidate at Nanyang Technological University. He received his BEng (Hons) degree in bioengineering at the same university in 2010. His current research interests include optical fiber sensors, optoelectronic systems, and bioinstrumentation.

Chi Chiu Chan is a professor at the School of Chemical and Biomedical Engineering, Nanyang Technological University. He received his BEng (Hons) and PhD degrees from the Department of Electrical Engineering, Hong Kong Polytechnic University in 1996 and 2000, respectively. His research areas include optical fiber sensing systems, fiber Bragg grating devices, fiber optics chemical sensors, photonic crystal fiber biosensors, and digital signal processing. His accomplishment in these areas is demonstrated in over 200 international publications.

Jesmond Hong received his BEng (Hons) degree in bioengineering from Nanyang Technological University, School of Chemical and Biomedical Engineering, in 2013. She is currently a PhD candidate.

Shermaine Png received her BEng (Hons) degree in bioengineering from Nanyang Technological University, School of Chemical and Biomedical Engineering, in 2013. She is currently a project engineer at Biosensors International.

Khay Ming Tan Eddie received his BEng (Hons) degree in electrical and electronic engineering from Nanyang Technological University in 2002. He graduated with a PhD from the same university in 2007. During his PhD, he researched long period fiber grating and fiber Bragg gratings for sensors applications. He has published numerous papers in international peer-reviewed journals and conferences. He is currently with Einst Technology Pte Ltd. (Singapore) as an application scientist researching and developing solutions in the area of Raman spectroscopy and optical fiber sensors.

Terence Aik Huang Tan is a medical oncologist and founder of OncoSolutions Cancer Center. He is currently a postdoctoral research fellow at Nanyang Technological University, School of Chemical and Biomedical Engineering, Division of Bioengineering, Singapore. His translational research interests lie at the interface of genomics, informatics, and bioengineering, and he actively collaborates with an interdisciplinary team of bioengineers, cancer scientists, and bioinformaticians to develop novel devices for a new era of precision cancer medicine.